

Englerin A Inhibits EWS-FLI1 DNA Binding in Ewing Sarcoma Cells*

Received for publication, October 29, 2015, and in revised form, March 3, 2016 Published, JBC Papers in Press, March 9, 2016, DOI 10.1074/jbc.M115.701375

Vittorio Caropreso[‡], Emad Darvishi[‡], Thomas J. Turbyville[§], Ranjala Ratnayake[‡], Patrick J. Grohar[¶], James B. McMahon[‡], and Girma M. Woldemichael^{**1}

From the [‡]Molecular Targets Laboratory, NCI, National Institutes of Health, [§]Optical Microscopy and Analysis Laboratory, Leidos Biomedical Research, Inc., and ^{**}Basic Science Program, Leidos Biomedical Research, Inc., Molecular Targets Laboratory, Frederick National Laboratory, Frederick, Maryland 21702, [¶]Center for Cancer and Cell Biology, Van Andel Institute, Grand Rapids, Michigan 49503, and ^{||}Division of Hematology/Oncology, Helen DeVos Children's Hospital, Grand Rapids, Michigan 49503

High-throughput screening of extracts from plants, marine, and micro-organisms led to the identification of the extract from the plant *Phyllanthus engleri* as the most potent inhibitor of EWS-FLI1 induced luciferase reporter expression. Testing of compounds isolated from this extract in turn led to the identification of Englerin A (EA) as the active constituent of the extract. EA induced both necrosis and apoptosis in Ewing cells subsequent to a G2M accumulation of cells in the cell cycle. It also impacted clonogenic survival and anchorage-independent proliferation while also decreasing the proportion of chemotherapy-resistant cells identified by high ALDH activity. EA also caused a sustained increase in cytosolic calcium levels. EA appears to exert its effect on Ewing cells through a decrease in phosphorylation of EWS-FLI1 and its ability to bind DNA. This effect is mediated, at least in part, through a decrease in the levels of the calcium-dependent protein kinase PKC- β I after a transient up-regulation.

The hallmark that defines the Ewing sarcoma family of tumors is the presence of non-random chromosomal rearrangements between the Ewing sarcoma breakpoint region 1 gene (EWS)² located on chromosome 22q12 and genes of the E26 transformation-specific sequence (ETS) family of transcription factors. Reciprocal chromosomal translocations, t(11;22)(q24;q12), that result in the fusion of the transactivational domain of EWS and the DNA binding domain of FLI1, an ETS transcription factor, generating the chimeric EWS-FLI1 fusion transcript underlie an overwhelming majority of cases of Ewing sarcoma (1). The disease arises in less than 3 per million people

under the age of 20, with 90% of all cases being found in patients between 5 and 25 years of age (2). Prior to the advent of chemotherapy, up to 90% of patients succumbed to the disease when only surgery and/or radiation were used. Current standard treatment constitutes combination chemotherapy along with surgery and/or radiation. This approach has had a positive impact on event-free survival and overall survival. However, in 27% of patients diagnosed with localized disease, this treatment modality still fails to improve overall survival (3). Furthermore, 15–25% of patients present with metastases upon diagnosis and the cure rate among this group is below 20% (4). Overall the long-term cure rate in children and adolescents with Ewing sarcoma still remains under 60% (5). Various reports show the aberrant transcription factor EWS-FLI1 is a key contributor in the tumorigenesis and progression of Ewing sarcoma (6, 7). The discovery of molecules that modulate its activity are expected to not only provide a better understanding of the biology behind the disease but are also expected to lead to the development of chemotherapeutic agents targeting the disease. Herein we describe results from a mode-of-action study undertaken using a compound identified as an inhibitor from a plant extract in a primary high-throughput screen (HTS).

Experimental Procedures

Reagents—Synthetic EWS-FLI1 siRNA were AGCAGAAC-CCUUCUUAUGACUU (sense) and GUCAUAAGAAGGGU-UCUGCUUU (antisense) (8). RNAi directed at TRPC4 (sc-42668) and TRPC5 (sc-42670) were commercially obtained from Santa Cruz Biotechnologies. Q-VD-Oph (SML006) and ML204 (SML0400) were obtained from Sigma-Aldrich. A portion of the EA used in the study was obtained via isolation from extracts of *Phyllanthus engleri* (9). Additional EA was commercially obtained from Cerilliant (PHY82530). EWS-FLI1 expression plasmid pcDNA3.1 EWS-myc-HIS was a gift from Heinz Gehring (Addgene plasmid # 46386) while generation of the phosphorylation mimetic serine 266 to aspartic acid (S266D) and phosphorylation-deficient serine 266 to alanine (S266A) by site directed mutagenesis has been described previously (10). Constitutively active Akt plasmid was a gift from Richard Roth (Addgene plasmid #10841), while that for constitutively active Erk was a gift from Melanie Cobb (Addgene plasmid #39197).

Cells and Culture Conditions—Growth and propagation conditions and characterization of TC32 cells have been described previously (11). EW8 and 5838 cells were obtained from Dr. Lee

* This research was supported in part by the Intramural Research Program of National Institutes of Health, Frederick National Lab, Center for Cancer Research. It has also been funded in part with federal funds from the Frederick National Laboratory for Cancer Research, National Institutes of Health, under contract HHSN261200800001E. The content of this publication does not necessarily reflect the views or policies of the Dept. of Health and Human Services, nor does mention of trade names, commercial products or organizations imply endorsement by the US Government. The authors declare that they have no conflicts of interest with the contents of this article.

¹ To whom correspondence should be addressed: Molecular Targets Laboratory, Frederick National Lab, Bldg. 538, Rm 131, 1050 Boyles St., Frederick, MD 21702. Tel.: 301-846-5578; E-mail: woldemichaelg@mail.nih.gov.

² The abbreviations used are: EWS, the Ewing sarcoma breakpoint region 1 gene; EA, Englerin A; HTS, high throughput screening; ALDH, aldehyde dehydrogenase; TRPC, transient receptor potential canonical calcium channel; TF, transcription factor.

Helman of the Pediatric Oncology Branch, NCI, National Institutes of Health, whose laboratory performed authentication of the cell lines by short-tandem repeat genotyping. All other cell lines were obtained from ATCC. Throughout their use, cell morphology, growth curve, and possible mycoplasma contamination were regularly monitored.

Transcription Factor Activity Profiling—200 ng of a luciferase transcription factor reporter or the negative control (construct with a minimal promoter) or the positive control (CMV driven luciferase reporter) along with 9.5 ng of a normalization reporter construct (CMV-driven *Renilla* luciferase reporter) and 1.2 μ l of transfection reagent in 100 μ l of Opti-mem (Gibco, 11058) medium per well were used. Cells were seeded into each well of a 96-well plate containing 100 μ l of the transfection mixture by adding 4×10^5 cells in 50 μ l Opti-mem media containing 10% FBS and 1% non-essential amino acids (NEAA). After incubation for 24 h, medium in each well was replaced with 75 μ l of medium composed of Opti-mem, 0.5% FBS and 1% NEAA and containing either the test compound or DMSO as a control. After a further 24-h incubation, dual luminescence in plates was read using Dual-Glo reagent (Promega, E2920). Data for each transcription factor was generated in quadruplicate and is shown as average \pm standard error of three independent experiments.

Western Blot Analysis—Cells were lysed with Nonidet P-40 lysis buffer (Life Technologies, FNN0021) containing PMSF (Sigma P7626) and protease inhibitor cocktails (Thermo, 78430). Total protein concentrations in lysates were determined using the BCA assay (Thermo, 23228, 1859078). 30 μ g of protein from lysates was separated by SDS-PAGE, transferred to nitrocellulose membranes, blocked overnight in Odyssey blocking buffer (Li-Cor, 927-40000) at 4 °C, and incubated with primary antibodies, p-AKT (4060, 2965), AKT (4691), p-Erk1/2 (4377), Erk1/2 (9102), cleaved caspase-3 (9661) obtained from Cell Signaling, p21 (sc-756), NKX2.2 (sc-15015), CAV-1 (sc-894) from Santa Cruz Biotechnology, PHLDA1 (ab133654) from Abcam and NR0B1 (554002) from BD. After incubating with primary antibodies, membranes were washed and incubated with anti-mouse IRDye 680 (926–32221) and anti-rabbit IRDye 800 (926–32210)-conjugated secondary antibodies (Li-Cor). Blots were scanned using Odyssey infrared imaging system. Intensities of bands of interest were normalized to the corresponding signals from the loading control bands of β -actin, α -tubulin, or GAPDH. In addition, band intensities were determined using the Odyssey band quantitation software Image Studio after background subtraction.

Flow Cytometry Analysis—For cell cycle analysis, TC32 and A673 (3×10^6 cells) cells were incubated in the presence or absence of 1 nM EA for 24 h. At the end of this period, BrdU (BD, #552598) was added at 10 μ M final concentration, and cells were incubated for an additional 45 min. After trypsinization and washing with ice-cold 2% FBS in PBS, cells were fixed, permeabilized, and incubated with DNase (1 h) and RNase (15 min) at 37 °C. Next, cells were incubated with APO-labeled anti-BrdU antibody for 20 min at room temperature. Finally, cells were washed and labeled with 7-AAD prior to flow cytometry.

TC32 and A673 (3×10^6 cells) cells were also incubated in the presence or absence of 1 nM EA for 48 h to determine effect of EA on ALDH or CD133-positive cells. The Aldefluor assay kit (Stemcell Technologies, #01700) and CD 133 antibody (Miltenyi Biotec, #130-105-225) were used following the vendor's suggested protocol. Cells with high ALDH activity were identified via comparison of untreated samples to those treated with the ALDH inhibitor DEAB. 10,000 events each were acquired using a BD Accuri C6 flow cytometer. Dead cells were excluded by staining with 7-AAD immediately prior to analysis. The assay was performed in quadruplicate with two independent experiments.

Clonogenic Assay and Growth in Methyl Cellulose and Soft Agar—Cells were treated with increasing concentration of EA for 24 h. After harvesting, cells were seeded at 100 cells/dish in 60-mm dishes in complete medium and allowed to grow for 14 days. Colonies were fixed and stained with crystal violet. About 3×10^4 each of TC32 and A673 cells suspended in 1.2 ml of medium were mixed with an equal volume of either 10 nM EA or DMSO in medium. These were added to 9.6 ml of methylcellulose matrix (03814, StemCell Technologies). 2 ml of this mixture was plated into agar-precoated grided-6 cm plate and incubated for 10 days. Colonies from 100 squares were counted using a microscope. Each condition was run in triplicate while three independent experiments were performed. For soft agar colony formation assay, wells in a 24-well plate were coated with 0.5 ml of the bottom agar mixture (10% fetal bovine serum, DMEM, and 0.6% agar). After the bottom layer had solidified, 0.5 ml of the top agar mixture (10% fetal bovine serum, DMEM, and 0.3% agar) containing 1500 cells/well and either 2 nM (1 nM final concentration) of EA or DMSO (control) was added into each well. Plates were incubated for 3 weeks. Colonies were visualized at 20 \times magnification, manually counted, and the average number of colonies per well was calculated. Data is reported as means \pm S.E. of three independent experiments. Statistical differences were evaluated using the Student's *t* test, with a *p* value < 0.001 considered statistically significant.

Cell Viability, Apoptosis, and Necrosis Assays—Cell viability was assessed using XTT reduction to a colored formazan product with absorbance measurements in 384-well plates as described previously at 24-h post treatment (12). Measurement of total ATP content using a luminescence assay (Promega, G7570) allowed inference of effect on cell viability against a panel of 19 cell lines treated with 10-fold serial dilutions of EA (100 μ M to 0.0001 nM) in quadruplicate or with DMSO for 72 h. The half maximal effective concentration (EC₅₀) values were then calculated from the data using Graphpad Prism 6. Fluorescence microscopic studies to detect necrotic effects were carried out in 96-well plates containing 30,000 cells per well and using a BioTek Cytation 3 high content imager with a 40 \times objective. After treatment, cells were double-stained using 10 μ M Hoechst 33342 (H1399, Life Technologies,) and 10 μ M propidium iodide (Life Technologies, P21493) for 3 min prior to imaging. Necrotic cells were identified based on positive staining with both propidium iodide (PI) and Hoechst 33342 and absence of nuclear fragmentation. Each plate contained 8 replicates per condition, and two independent experiments were performed.

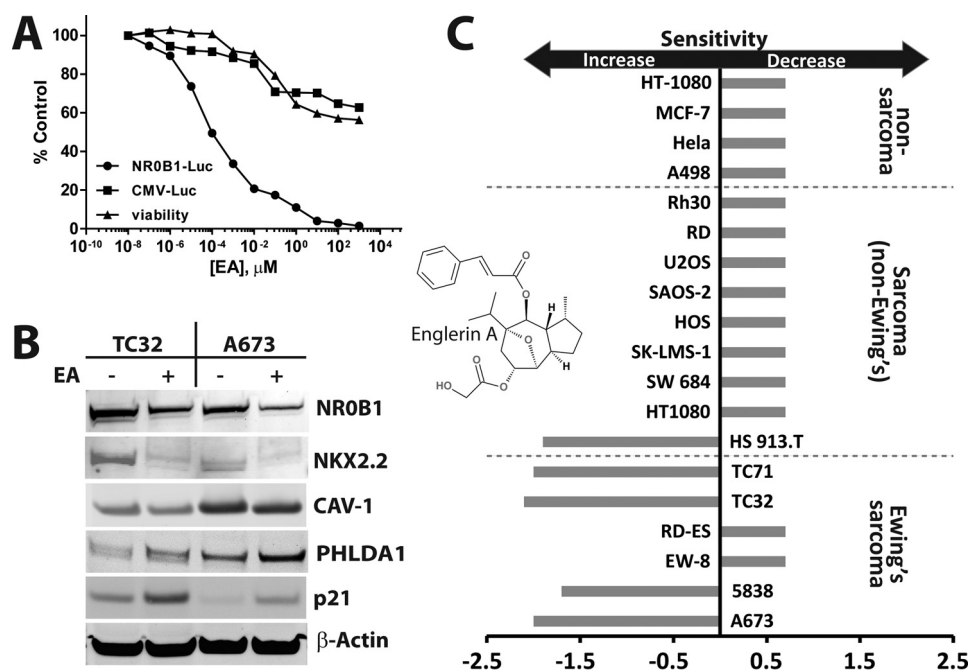


FIGURE 1. EA inhibits EWS-FLI1 activity. A, EA is a potent inhibitor of EWS-FLI1 driven reporter expression in a dose-dependent manner (NR0B1-Luc) while inhibiting general transcription (CMV-Luc) and cell viability only at 100- to 1000-fold higher concentrations at 24 h. B, EA induces changes at the protein level of genes that are both up- and down-regulated by EWS-FLI1. Lysates for Western blotting were prepared 24 h after cells were treated with 1 nM EA. C, EA shows selective activity against Ewing sarcoma cell lines. Data are shown as difference of LogEC₅₀ values for EA in each cell line from mean of all Log(EC₅₀) values measured 72 h after treatment.

Calcium Orange Assay—Cells were seeded in 96-well plates and treated either with DMSO (control) or 1 nM EA for 0, 3, 7, 24, and 48 h. Stock solution of Calcium Orange-AM (Life Technologies, C-3015), 0.82 mM containing 20% pluronic F-127 (P-6867) in DMSO, were diluted to 1 μ M in Ca²⁺-free PBS to prepare the loading solution. After washing wells with Ca²⁺-Mg²⁺-free PBS, cells were loaded with calcium orange by incubating with the loading solution at room temperature for 30 min. After removing the loading solution and washing, images of cells in wells were acquired using a Nikon T2000S fluorescence microscope with a 20 \times objective.

Quantitative Real Time PCR—To compare the expression of wild-type EWS-FLI1 and either S266D or S266A myc-tagged mutants in TC32 cells, total RNA was extracted using an RNeasy kit (Qiagen, #74106). About 2 μ g of this RNA was used for analysis. EWS-FLI1, β -actin, and HSP90 probes used for qRT-PCR were obtained commercially (ThermoFisher, Hs03024497_ft, Hs00969077_g1, Hs00427665_g1). Probes for S266D and S266A EWS-FLI1 mutants, forward 5'-ATGCCTGTCCTTCCTCCAG-3' and reverse 5'-GCACGTGGGTGTTAGGATG-3', were designed to include the 3'-myc-tag.

Electromobility Shift Assay—Nuclear protein extracts were prepared from control and EA-treated A673 and TC32 cells using a commercial kit (Abcam, ab113477) and 1.25 μ g of nucleic acid-free total nuclear protein extract was used per reaction. Oligonucleotide sequences for 5' IRDye700-tagged EWS-FLI1-binding and non-binding probes used were 5'-CCTGAAACAGGA-AGTCAGTCAG-3' (EWS-FLI1 IR-probe) and 5'-CCCTTGCCTTGAGATCAGAATT-3' (EWS-FLI1 non-binding IR-probe, lacking the GGAA Ets transcription factor binding motif (13)), respectively. Double-stranded oligonucleotide probes were generated by annealing equimolar com-

plementary oligonucleotides via heating for 3 min at 95 $^{\circ}$ C and controlled cooling to room temperature over 90 min. For competition assays, 100-fold excess EWS-FLI1-binding double-stranded probe (untagged with IRDye700 label) was used. Samples were loaded onto a 4–20% acrylamide gel and run in a Tris borate-EDTA (TBE) buffer for 90 min. Following this, gels were dry-blotted onto Nylon membranes, and membranes were scanned using an Odyssey infrared imager.

Results

High Throughput Screening Identifies EA as an Inhibitor of EWS-FLI1 Activity—A high throughput screen (HTS) developed using the Ewing sarcoma cell line TC32 stably transduced with a luciferase reporter construct that reports on EWS-FLI1 activity was used to screen over 60,000 natural products extracts (11). The top scoring extract in the primary screen was that of the African plant *Phyllanthus engleri*. Because of a concurrent interest in this extract stemming from an unrelated NCI60 cell screen at the time and the identification of an apparent selective activity against renal carcinoma cells (14), bioassay-guided fractionation enabled the identification of sesquiterpenes as its bioactive constituents (9). Testing these sesquiterpenes in TC32 cells with a luciferase reporter for EWS-FLI1 activity allowed the identification of englerin A (EA) as the active constituent of the extract with other constituents of the extract (including other englerins) showing no activity. EA inhibited EWS-FLI1-induced luciferase reporter expression with an IC₅₀ of less than 1 nM at 24 h (Fig. 1A). Its inhibitory effects on general transcription, on the other hand, largely parallel its effect on cell proliferation. Further confirmation for EA effect on EWS-FLI1 activity was obtained by looking at the levels of three proteins whose expression is driven by EWS-FLI1

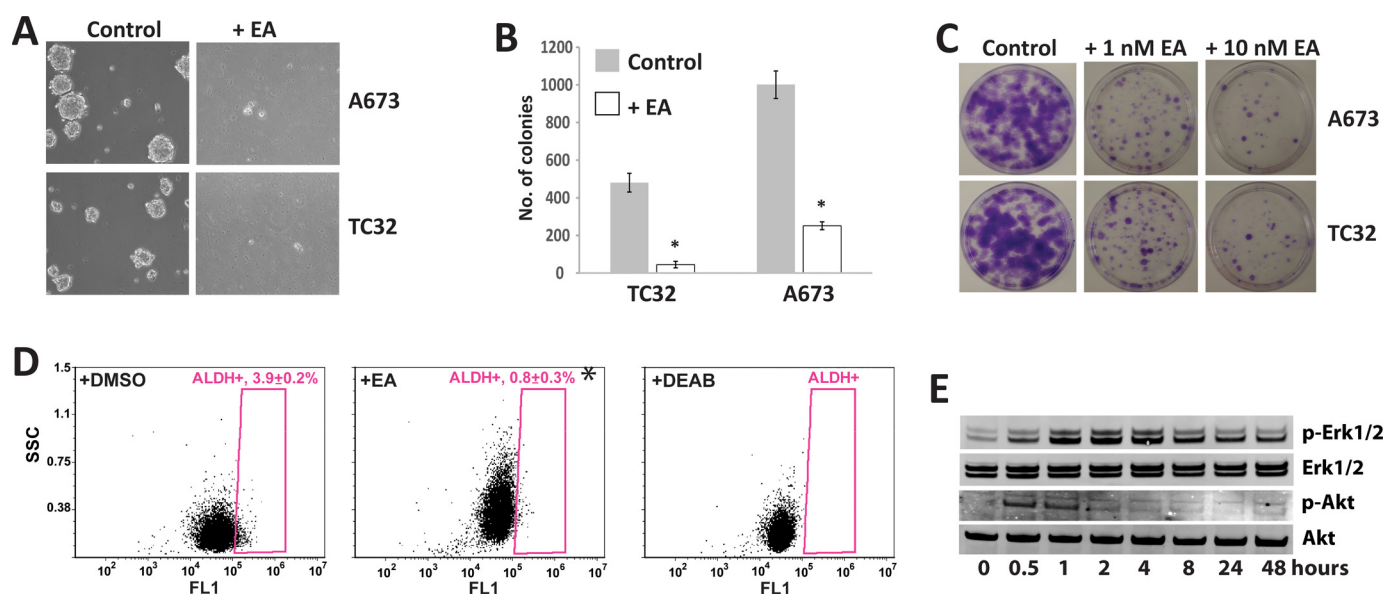


FIGURE 2. EA inhibits anchorage-independent and clonogenic growth. A, TC32 and A673 Ewing cells were incubated in a methyl cellulose matrix in the presence of either DMSO (control) or EA (1 nM). Shown are representative images. B, EA was a potent inhibitor of colony formation by Ewing cells in soft agar. Results are mean \pm S.E. of three independent experiments. Asterisks indicate statistically significant differences between treatments (*, $p < 0.001$). C, clonogenic survival assay representative images showing EA reduced clonogenic survival of Ewing cells A673 and TC32 pretreated for 24 h prior to seeding. D, A673 cells were treated with Aldefluor reagent alone, with EA (1 nM) for 48 h or the ALDH inhibitor DEAB (15 μ M) shortly before testing. Flow cytometry analysis shows that EA treatment decreased the proportion of ALDH-positive cells (*, $p < 0.01$). E, time course Western blotting for Akt and Erk activation by EA (1 nM). Treatment induces activation of ERK subsequent to transient Akt activation.

activity- NKX2.2, caveolin 1 (CAV1), and NR0B1 (15–17). We also looked at levels of two proteins, PHLDA1 and p21^{WAF1/CIP1}, whose expression is suppressed by EWS-FLI1 in Ewing cells (18, 19). We found levels of CAV1, NKX2.2, and NR0B1 decreased while PHLDA1 and p21^{WAF1/CIP1} (with no accompanying change in p53) levels increased in response to treatment with EA (Fig. 1B). Assessment of its impact on cell viability against a panel of cell lines, including other sarcoma cell lines and cell lines with differing tissues of origin, showed that it inhibited proliferation with a mean EC₅₀ of about 16 μ M for all tested cell lines at 72 h while showing an EC₅₀ of less than 100 nM in four of the six tested Ewing cell lines, suggesting that it possesses selective activity against Ewing cells (Fig. 1C). Together, these results suggest that EA not only impacts EWS-FLI1 activity but that it also possesses selective antiproliferative effect against Ewing cells.

EA Treatment Correlates with Decreased Tumorigenicity in Ewing Cells—Because EA had a strong anti-proliferative effect on Ewing cells under culture conditions, its impact on anchorage-independent proliferation and clonogenic survival, both hallmarks of Ewing tumor cells, were investigated. Anchorage-independent growth assay performed in a methylcellulose matrix and tumor sphere formation measured in soft agar with TC32 and A673 cells both showed that EA significantly inhibited these properties (Fig. 2, A and B). Measurement of clonogenic survival in EA treated TC32 and A673 cells also similarly showed that it was impacted in a dose-dependent manner (Fig. 2C). High ALDH activity has been used to identify chemotherapy-resistant Ewing cells that are capable of clonogenic survival (20). On average, EA treatment reduced the percentage of ALDH positive cells by more than 4-fold relative to control treatment (Fig. 2D). Impact by EA on CD133-positive populations was also assessed as it has been reported as being a

marker for tumor initiating cells in Ewing sarcoma family of tumors (21). The results showed that EA did not alter the percentage of CD133-positive TC32 cells ($4.2\% \pm 0.78\%$, mean \pm S.E.) relative to DMSO treatment while the positive control used, doxorubicin at 500 nM, increased the CD133-positive population ($9.5\% \pm 0.42\%$, mean \pm S.E., $p < 0.05$) relative to DMSO treatment.

IGF-related autocrine loops play a crucial role in the tumorigenesis and progression of Ewing sarcoma *in vivo* and proliferation and survival of Ewing cells *in vitro* predominantly via activation of AKT and to a lesser extent through ERK1/2 (22). Because of EA's antiproliferative effect on Ewing cells, we also asked whether its impact on proliferation was mediated through inhibition of these key signaling molecules. As shown in Fig. 2E, AKT signaling was up-regulated soon after treatment with EA. Continued exposure, however, resulted in attenuation of p-AKT levels. Similarly, p-ERK levels can also be seen to be transiently up-regulated. Pre-treatment of cells with either insulin or IGF-1 did not rescue cells from EA's effects. Transient transfection experiments with constitutively active AKT and ERK1/2 isoforms also similarly failed to rescue Ewing cells from the antiproliferative effects of EA. The transient AKT and ERK activation responses by Ewing cells, therefore, appear to be immediate pro-survival responses to EA's antiproliferative effects that these cells are ultimately unable to overcome.

Ewing Cells Treated with EA Undergo Cell Cycle Arrest and Cell Death—Direct observation of EA treated cells under the microscope showed that treatment induced cell rounding and detachment in some cells. Flow cytometry analysis of cells that remained adherent after EA treatment showed accumulation of cells in G2M phases of the cell cycle of cells double labeled with bromodeoxy-uridine (BrdU) and 7-amino-actinomycin D (7-AAD) (Fig. 3A). Furthermore, double staining of cells that

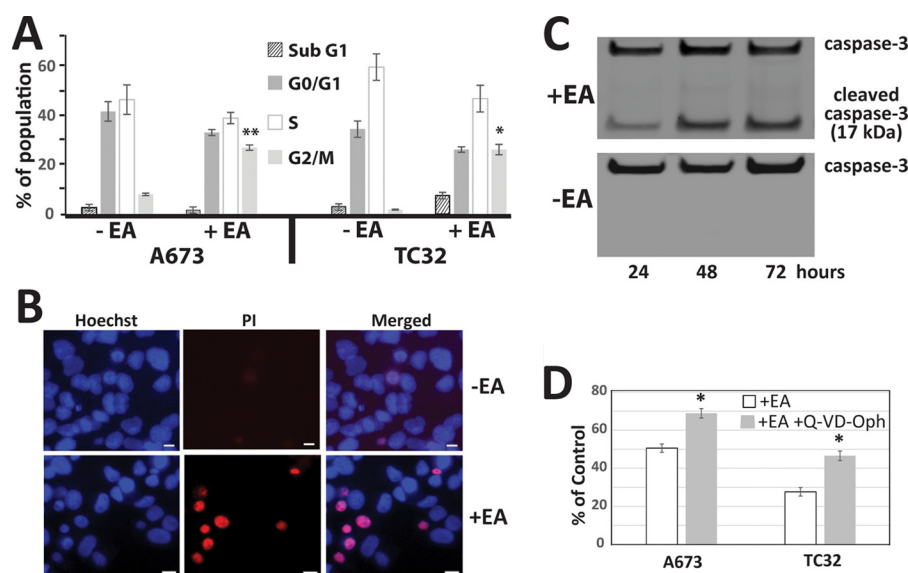


FIGURE 3. EA induces cell cycle arrest and cell death. *A*, flow cytometry analysis of control and EA treated A673 and TC32 Ewing cells showed accumulation of cells in the G2/M phases of the cell cycle in cells that remained adherent 24 h after treatment with 1 nM EA. Results shown are means of three independent experiments (*, $p < 0.001$; **, $p < 0.01$). *B*, representative images of cells double-stained with Hoechst 33342 (blue) and PI (red) 48 h after treatment with 1 nM EA. TC32 cells were treated as shown in the figure and imaged (40 \times magnification, 10 μ m bars). Nuclei of viable cells appear stained only in blue. Necrotic cells appear with normal nuclei stained red in the PI channel and appear purple (double-stained) in the merged image. *C*, cells that detached after treatment with EA (1 nM) were collected at the time points shown and protein lysates extracted were subjected to Western blotting for caspase-3 activation. The results show that EA restores anoikis response in Ewing cells. *D*, pretreatment of TC32 and A673 cells with the pan caspase inhibitor Q-VD-Oph partially reversed EA (1 nM) cell viability effects. Cell viability was measured using XTT reduction to a colored formazan product using absorbance. Results shown are means of three independent experiments relative to DMSO treatment (*, $p < 0.01$).

remained adherent with Hoechst 33342 and propidium iodide (PI) revealed that, EA increased the number of necrotic cells (Fig. 3*B*) relative to control treatment ($33.6\% \pm 4.42\%$, mean \pm S.E., $p < 0.05$) while timecourse experiments revealed no activation of caspases-1/3/7/8/9/12. Caspase-3 activation, on the other hand, was clearly evident in cells that detached (Fig. 3*C*). Pretreatment of cells with the pan-caspase inhibitor Q-VD-Oph only partially reversed EA's effect on cell viability suggesting that EA induces cell cycle arrest and necrotic cell death in cells that remain adherent while triggering apoptotic cell death in cells that detach (Fig. 3*D*).

EA Treatment Increases Cytosolic Calcium Levels—To get a clearer picture of signaling pathways that are involved in mediating EA effects, we undertook transcription factor (TF) activity profiling of treated cells transiently transfected with luciferase reporters for various TFs. Because some impact on cell viability only became detectable 24 h after treatment with EA, a TF activity profile was generated at this time point. The results showed that EA treatment resulted in an increased reporter activity by heat-shock (HSE), cyclic AMP (CRE), and AP-1 TF reporters, with the Hedgehog TF (GLRE) reporter showing the most significant decrease in reporter activity in both TC32 and A673 cells (Fig. 4*A*). This activity profile was suggestive of changes in Ca^{2+} homeostasis and/or signaling (23–26). Interestingly, previous high throughput screens aimed at identifying inhibitors of Fli-1 in leukemia led to the identification of calcium ionophores including calcimycin and thapsigargin as hits (27). Calcimycin and thapsigargin were also found to moderately inhibit EWS-FLI1 induced luciferase reporter activity in our screen suggesting that EA may also exert its effects through modulation of intracellular calcium levels. As a result, changes in intracellular calcium levels were monitored using the fluo-

rescent calcium ionophore calcium-orange over a 48 h period. Time course images acquired after treatment with EA revealed an increase in free cytosolic Ca^{2+} levels (Fig. 4*B*). A recent report on EA's effects in renal carcinoma cell viability suggested that it may exert its effects through a direct and selective activation of transient receptor potential canonical calcium channels 4 and 5 (TRPC4/C5) (28). Pretreatment of Ewing cells with combined siRNAs targeting TRPC4/C5 was lethal to all tested Ewing cell lines. Knockdown of TRPC4 (but not of TRPC5) alone attenuated EWS-FLI1 activity while not altering sensitivity to EA's effect on EWS-FLI1 driven reporter activity. On the other hand, pretreatment with ML204, a selective inhibitor of TRPC4/5 channels, showed that ML204 attenuated EWS-FLI1 activity in TC32 cells in a dose-dependent manner (Fig. 4*C*) (29). Together, these findings point to an effect on calcium channels by EA in mediating an increase in cytosolic calcium levels and suggest a correlation between increased cytosolic calcium levels and inhibition of EWS-FLI1 activity.

EA Decreases EWS-FLI1 Phosphorylation and DNA Binding—Although EA inhibits EWS-FLI1 driven luciferase reporter expression, it showed no impact on total EWS-FLI1 protein levels in Ewing cells in Western blotting experiments. Therefore, we looked at potential interactions between calcium signaling and EWS-FLI1 activity. Experiments with the calcium chelator ethylene glycol tetraacetic acid (EGTA) provided evidence for a link between calcium influx into cytosolic compartments and modulation of EWS-FLI1 activity in that depletion of extracellular calcium with EGTA significantly attenuated the inhibitory effect of EA on EWS-FLI1 induced luciferase expression in TC32 reporter cells (Fig. 5*A*). Previous studies have found that phosphorylation of the EWS fragment in EWS-FLI1 and EWS-WT1 fusions is a major regulator of their DNA rec-

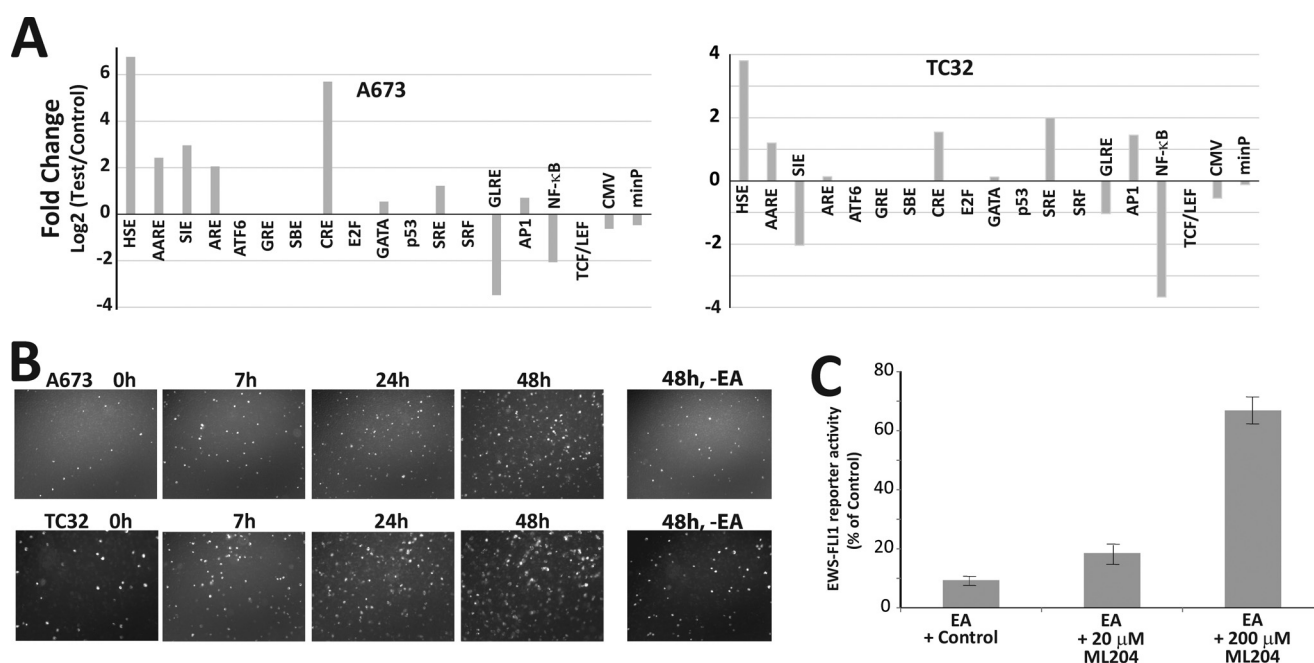


FIGURE 4. EA increases cytosolic calcium levels. *A*, in a transient reporter transfection assay, EA (1 nM) treatment caused the activation of transcription factors involved in the regulation of intracellular calcium levels. *B*, time course incubation of Ewing cells with the cell permeant ester calcium orange AM, which is cleaved inside cells trapping it. The pictures show an increase in intracellular fluorescence over time when Ewing cells are treated with 1 nM EA. *C*, pretreatment of EWS-FLI1 luciferase reporter cells with the TRPC4/C5 Ca^{2+} channel inhibitor compound ML204 attenuated inhibitory effects of (1 nM) on EWS-FLI1 activity in TC32 cells.

ognition and binding and to a lesser extent their nuclear localization and that this phosphorylation, in turn, is modulated by intracellular calcium levels (10, 30, 31). However, chronic elevated cytosolic calcium levels by cell permeant calcium ionophores are known to decrease the kinase activity of calcium induced kinases (32). To identify calcium dependent kinases that may be involved in the phosphorylation of EWS-FLI1, a panel of 90 known small molecule protein kinase inhibitors were screened. Ruboxistaurin, rottlerin, and PKC-412 showed selective inhibition of EWS-FLI1 driven luciferase reporter activity relative to constitutively driven reporter expression in TC32 cells (Fig. 5B). All compounds are known inhibitors of protein kinase C with ruboxistaurin being a specific inhibitor of the β -isoform (33, 34). As a result, we looked at the impact of EA on calcium-dependent PKC isozymes. Western blotting of lysates from EA-treated cells showed a transient up-regulation of PKC- β I (Fig. 5C). No change in the levels of PKC- β II and PKC- γ was seen while PKC- α was not detected. On the other hand, Western blotting of EWS-FLI1 pulled-down from lysates of TC32 cells transiently transfected with a HIS-tagged EWS-FLI1 revealed that EA treatment reduced serine and threonine phosphorylation of EWS-FLI1 (Fig. 5D). Knock-down of PKC- β I using siRNA in TC32 cells transiently transfected with a HIS-tagged EWS-FLI1 similarly induced serine dephosphorylation of EWS-FLI1 protein (Fig. 5E). Transient transfection experiments setup with phosphorylation mimetic (S266D) and deficient (S266A) mutants of EWS-FLI1 showed that while the expression of the S266D mutant reduced EA ability to inhibit EWS-FLI1 induced luciferase reporter activity in TC32 luciferase reporter cells, the phosphorylation-deficient S266A mutant had no effect (Fig. 5, F and G). On the other hand, results from both Western blotting of nuclear and cytosolic protein frac-

tions as well as imaging experiments in cells with a GFP-tagged EWS-FLI1 showed no impact on nuclear/cytosolic localization of EWS-FLI1.

Evaluation of nuclear extracts from control and EA-treated A673 and TC32 cells in an electrophoretic mobility assay using an infrared dye labeled probe containing a consensus FLI1 binding sequence to capture nuclear EWS-FLI1 showed that EA treatment resulted in a significant decrease in DNA binding ability of nuclear EWS-FLI1 (Fig. 5H). On the other hand, inhibition of direct DNA binding experiments with EA using HIS-tagged EWS-FLI1 protein expressed in and purified from Ewing cells showed that EA had no appreciable inhibitory effects on direct binding between EWS-FLI1 and DNA when compared with DMSO control. Mithramycin used as positive control showed significant inhibition of direct binding. Together, the above data suggest that EA-induced sustained elevated cytosolic calcium levels play a role in decreasing phosphorylation of EWS-FLI1 and inhibit its DNA binding.

Discussion

The aberrant EWS-FLI1 TF represents an attractive target for therapeutics discovery efforts because it is only found in cells of Ewing tumors. Its inhibition using RNA interference and antisense DNA has been shown to impact cell proliferation *in vitro* and tumorigenesis *in vivo* in mouse models (35–37). However, like all TFs, it has traditionally been regarded as too difficult to target. As evidenced by the clinical utility of drugs targeting the nuclear-hormone-receptor family of TFs, discovery of inhibitors of EWS-FLI1 is feasible. Novel approaches to targeting EWS-FLI1 will, however, be needed. Our studies were carried out to contribute to filling the gap in understanding and targeting the biology behind EWS-FLI1-driven Ewing sarcoma.

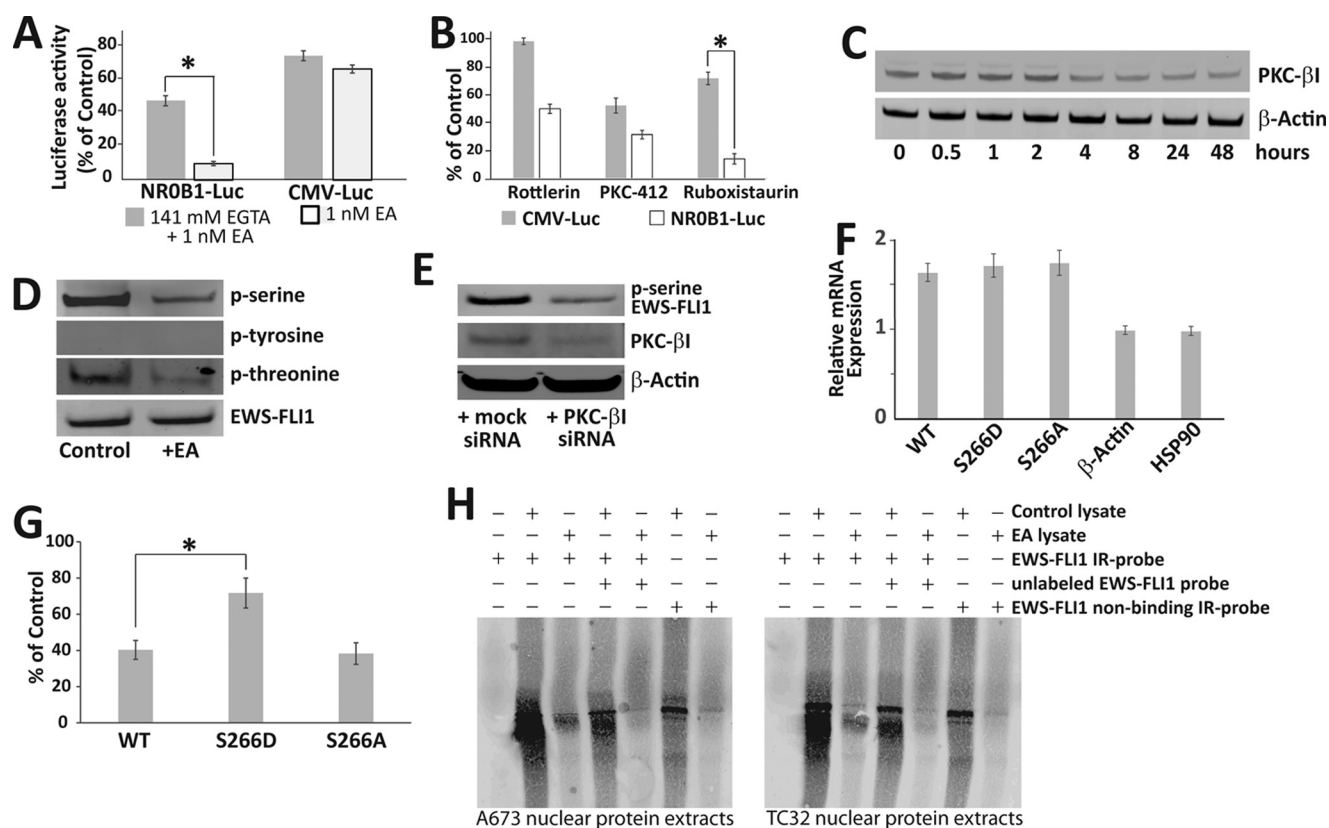


FIGURE 5. EA decreases EWS-FLI1 DNA binding. *A*, depletion of extracellular calcium using EGTA inhibits EWS-FLI1 driven luciferase reporter activity in TC32 NROB1-Luc cells. Results shown are means of three independent experiments (*, $p < 0.001$). *B*, screening of 90 known kinase inhibitors showed rottlerin, PKC-412 and ruboxistaurin all showed a differential inhibition of the EWS-FLI1 reporter 24h after treatment with 10 nM of each compound (*, $p < 0.01$). *C*, ScWestern blotting of calcium dependent protein kinase C (PKC) isozymes from 1 nM EA-treated TC32 cells showed a transient up-regulation of PKC- β I. *D*, HIS-tagged EWS-FLI1 was purified from DMSO (control) and 1 nM EA (+EA)-treated TC32 cells after 24 h and subjected to Western blotting. Probing blots with an antiphospho-serine/tyrosine/threonine antibodies shows a decrease in serine and threonine phosphorylation of EWS-FLI1 when comparable total EWS-FLI1 protein is loaded onto gels. *E*, siRNA knock-down of PKC- β I in TC32 cells is correlates with a decrease in serine phosphorylation of EWS-FLI1. EWS-FLI1 was purified using its his-tag prior to Western blot analysis. *F*, S266D and S266A mutant EWS-FLI1 are expressed to a comparable level as the wild-type (WT) in TC32 cells. *G*, TC32 luciferase reporter cells with wild type (WT) EWS-FLI1 were transiently transfected with an EWS-FLI1 phosphorylation mimic mutant (S266D). EA (1 nM) inhibition of reporter activity was attenuated by the S266D mutant after a 24-h incubation. Results shown are means of three independent experiments (*, $p < 0.01$). *H*, nuclear protein extracts of control and EA treated A673 and TC32 cells were subjected to EMSA with an EWS-FLI1 binding labeled oligo containing the EWS-FLI1 consensus sequence (lanes 1–5), an excess of unlabeled EWS-FLI1 binding oligo (lanes 4–5) for competition, or a non-binding labeled oligo (lanes 6–7). The difference in band intensities between control and treatment corresponds to lower levels of EWS-FLI1 protein in nuclei of EA-treated Ewing cells.

We set out with our discovery efforts by leveraging the power of high throughput screening and the mechanistic diversity of natural products (*i.e.* extracts and pure compounds derived from plants, marine and micro-organisms). The majority of currently known modulators of transcription factors are either natural products or are derived from them (38–42). Our choice of a natural products screening library for the discovery of an inhibitor of EWS-FLI1 is borne out not only by the identification of EA as an inhibitor but also by its mechanistic significance, *i.e.* a new approach to targeting EWS-FLI1 activity by small molecules.

Our results showed that EA was more selective in impacting viability of Ewing cells from among a panel of cell lines tested. We also found that, EA caused necrosis in Ewing cells that remained adherent after treatment while restoring anoikis like response in cells that detached after treatment. This is in contrast to previous reports showing that EA induces apoptosis in a number of cell lines. Although small changes in total cellular ATP content were apparent at 3h and 6h after treatment, monitoring of mitochondrial potential using JC-1 dye did not show

mitochondrial accumulation in cells that remained adherent after treatment. Results showing no change in the level or activation of proteins involved in apoptotic signaling stemming from the mitochondria (such as Bcl-2, p-Bad, and cytochrome *c*) were also consistent with a non-apoptotic cell death mechanism. Lack of any caspase activation and the absence of increased TUNEL staining also pointed to a non-apoptotic cell death mechanism for cells that remained adherent after EA treatment. We also found that EA did not increase oxidative stress. Autophagy induction in treated cells was ruled out based on the absence of fluorescently labeled vesicles in Ewing cells transfected with an expression construct for GFP tagged LC3B, an autophagosome component protein.

In many cases, the primary tumor in patients with Ewing sarcoma is chemoresponsive. Often, however, emergence of resistance to chemotherapy is a major contributor to morbidity in patients with metastases and recurring local disease. Studies by other groups have shown that a subpopulation of cells from human cell lines and xenografts identified by high ALDH activity possess traits such as resistance to therapeutic agents, clono-

genicity, sphere-formation, and tumor initiation. Our findings show that EA inhibited these traits while also decreasing the population of cells with ALDH activity. EA also did not result in an increase in the population of CD133 positive cells suggesting that these tumor-initiating cells are as sensitive as the rest of the population. IGF-I, a target gene of EWS-FLI1, is the principal growth factor produced by Ewing cells and its autocrine growth signaling is mediated by the PI3K/AKT and MAPK pathways (43, 44). These pathways are also involved in pro-survival responses seen in the development of resistance during chemotherapy (45). The discovery of inhibitors of EWS-FLI1 whose effects are not reversed by the emergence of chemotherapy resistance in Ewing tumors is, therefore, vital. Our results suggest that Ewing cells are unable to mount a sustained activation of the PI3K/AKT and MAPK pathways in response to EA. Furthermore, activation of these pathways through pretreatment with IGF-I or insulin or the expression of constitutively active AKT and ERK isoforms all failed to rescue Ewing cells from EA. Together, these findings not only show that it is possible to target EWS-FLI1 induced gene expression but also suggest that this may be done in a manner that overcomes emergence of drug resistance pathways mediated by PI3/AKT and MAPK.

EA was first discovered from extracts of the plant *P. engleri* because the extract showed renal cancer cell selectivity in an NCI-60 cell screen. Subsequent followup studies using renal carcinoma cells suggested that it exerts its effects through stimulation of PKC θ (46). However, unlike in renal carcinoma cells, siRNA knock down of PKC θ in Ewing cells rendered them even more sensitive to EA ruling it out as its target. Profiling the differential activity of a panel of transcription factors, on the other hand, enabled us to gain better insight into signaling pathways mediating EA effects in Ewing cells while suggesting a role for EA mediated changes in Ca²⁺ homeostasis and signaling in Ewing cells. Assays looking at changes in intracellular Ca²⁺ levels revealed a sustained increase in cytosolic Ca²⁺. However, Western blotting for markers of stress of the endoplasmic reticulum (the largest intracellular Ca²⁺ store), such as GRP78 and HSP70, showed no change in levels ruling out intracellular stores as the source. Inhibition of EWS-FLI1 driven reporter activity by the TRPC4/C5 inhibitor ML204 suggested that EA stimulates Ca²⁺ influx from extracellular sources. Inhibition of EWS-FLI1 driven luciferase expression by other specific TRPC inhibitors either largely paralleled cell toxicity or they had no effect. An interesting outcome of our HTS efforts was the identification of a number of hit compounds that are known modulators of intracellular calcium levels. In fact, mithramycin, which was our top scoring compound in our previous HTS effort with pure compounds, is a known modulator of calcium levels with a clinical application in the management of hypercalcemia.

Post-transcriptional modifications such as phosphorylation represent a significant mechanism regulating transcription factor induced gene expression. In this regard, our findings demonstrate that EA-induced Ca²⁺ influx into the cytosol inhibited PKC- β I expression. We also show that decrease in the levels of PKC- β I correlated with decrease in phosphorylation levels of EWS-FLI1. Whether PKC- β I directly phosphorylates EWS-FLI1 or is a component of a signaling pathway that culminates

in phosphorylation of EWS-FLI1 awaits further experimentation. That its inhibition either using siRNA or a small molecule resulted in decreased phosphorylation of EWS-FLI1, however, establishes a link with calcium signaling.

In conclusion, our findings suggest that inhibition of EWS-FLI1 activity and its DNA binding are affected by changes in cytosolic calcium levels and that this can be exploited for small molecule therapeutics discoveries in targeting Ewing sarcoma.

Author Contributions—G. M. W. and P. G. conceived and designed the experiments. V. C., G. M. W., E. D., and T. T. performed the experiments. V. C. and G. M. W. analyzed the data. J. B., T. T., R. R., and P. G. contributed reagents/materials/analysis tools. G. M. W., V. C., E. D., T. T., R. R., P. G., and J. M. wrote the paper.

References

1. Delattre, O., Zucman, J., Plougastel, B., Desmaze, C., Melot, T., Peter, M., Kovar, H., Joubert, L., de Jong, P., and Rouleau, G. (1992) Gene fusion with an ETS DNA-binding domain caused by chromosome translocation in human tumours. *Nature* **359**, 162–165
2. Esiashvili, N., Goodman, M., and Marcus, R. B., Jr. (2008) Changes in incidence and survival of Ewing sarcoma patients over the past 3 decades: Surveillance Epidemiology and End Results data. *J. Pediatr. Hematol. Oncol.* **30**, 425–430
3. Womer, R. B., West, D. C., Krailo, M. D., Dickman, P. S., Pawel, B. R., Grier, H. E., Marcus, K., Sailer, S., Healey, J. H., Dormans, J. P., and Weiss, A. R. (2012) Randomized controlled trial of interval-compressed chemotherapy for the treatment of localized Ewing sarcoma: a report from the Children's Oncology Group. *J. Clin. Oncol.* **30**, 4148–4154
4. Miser, J. S., Goldsby, R. E., Chen, Z., Krailo, M. D., Tarbell, N. J., Link, M. P., Fryer, C. J., Pritchard, D. J., Gebhardt, M. C., Dickman, P. S., Perlman, E. J., Meyers, P. A., Donaldson, S. S., Moore, S. G., Rausen, A. R., et al. (2007) Treatment of metastatic Ewing sarcoma/primitive neuroectodermal tumor of bone: evaluation of increasing the dose intensity of chemotherapy: a report from the Children's Oncology Group. *Pediatr. Blood Cancer* **49**, 894–900
5. Linabery, A. M., and Ross, J. A. (2008) Childhood and adolescent cancer survival in the US by race and ethnicity for the diagnostic period 1975–1999. *Cancer* **113**, 2575–2596
6. Leacock, S. W., Basse, A. N., Chandler, G. L., Kirk, A. M., Rakheja, D., and Amatruda, J. F. (2012) A zebrafish transgenic model of Ewing's sarcoma reveals conserved mediators of EWS-FLI1 tumorigenesis. *Dis. Model Mech.* **5**, 95–106
7. Kovar, H. (2010) Downstream EWS/FLI1 - upstream Ewing's sarcoma. *Genome Med.* **2**, 8
8. Nagano, A., Ohno, T., Shimizu, K., Hara, A., Yamamoto, T., Kawai, G., Saitou, M., Takigami, I., Matsushashi, A., Yamada, K., and Takei, Y. (2010) EWS/Fli-1 chimeric fusion gene upregulates vascular endothelial growth factor-A. *Int. J. Cancer* **126**, 2790–2798
9. Ratnayake, R., Covell, D., Ransom, T. T., Gustafson, K. R., and Beutler, J. A. (2009) Englerin A, a selective inhibitor of renal cancer cell growth, from *Phyllanthus engleri*. *Organic Letters* **11**, 57–60
10. Olsen, R. J., and Hinrichs, S. H. (2001) Phosphorylation of the EWS IQ domain regulates transcriptional activity of the EWS/ATF1 and EWS/FLI1 fusion proteins. *Oncogene* **20**, 1756–1764
11. Grohar, P. J., Woldemichael, G. M., Griffin, L. B., Mendoza, A., Chen, Q. R., Yeung, C., Currier, D. G., Davis, S., Khanna, C., Khan, J., McMahon, J. B., and Helman, L. J. (2011) Identification of an inhibitor of the EWS-FLI1 oncogenic transcription factor by high-throughput screening. *J. Natl. Cancer Inst.* **103**, 962–978
12. Woldemichael, G. M., Turbyville, T. J., Linehan, W. M., and McMahon, J. B. (2011) Carminomycin I is an apoptosis inducer that targets the Golgi complex in clear cell renal carcinoma cells. *Cancer Res.* **71**, 134–142
13. Guillon, N., Tirode, F., Boeva, V., Zynovyev, A., Barillot, E., and Delattre, O. (2009) The oncogenic EWS-FLI1 protein binds *in vivo* GGAA micro-

- satellite sequences with potential transcriptional activation function. *PLoS One* **4**, e4932
14. Shoemaker, R. H. (2006) The NCI60 human tumour cell line anticancer drug screen. *Nat. Rev. Cancer* **6**, 813–823
15. Owen, L. A., Kowalewski, A. A., and Lessnick, S. L. (2008) EWS/FLI mediates transcriptional repression via NKX2.2 during oncogenic transformation in Ewing's sarcoma. *PLoS One* **3**, e1965
16. Tirado, O. M., Mateo-Lozano, S., Villar, J., Dettin, L. E., Llorca, A., Gallego, S., Ban, J., Kovar, H., and Notario, V. (2006) Caveolin-1 (CAV1) is a target of EWS/FLI-1 and a key determinant of the oncogenic phenotype and tumorigenicity of Ewing's sarcoma cells. *Cancer Res.* **66**, 9937–9947
17. Kinsey, M., Smith, R., Iyer, A. K., McCabe, E. R., and Lessnick, S. L. (2009) EWS/FLI and its downstream target NR0B1 interact directly to modulate transcription and oncogenesis in Ewing's sarcoma. *Cancer Res.* **69**, 9047–9055
18. Nakatani, F., Tanaka, K., Sakimura, R., Matsumoto, Y., Matsunobu, T., Li, X., Hanada, M., Okada, T., and Iwamoto, Y. (2003) Identification of p21WAF1/CIP1 as a direct target of EWS-Flil oncogenic fusion protein. *J. Biol. Chem.* **278**, 15105–15115
19. Boro, A., Prêtre, K., Rechfeld, F., Thalhammer, V., Oesch, S., Wachtel, M., Schäfer, B. W., and Niggli, F. K. (2012) Small-molecule screen identifies modulators of EWS/FLI1 target gene expression and cell survival in Ewing's sarcoma. *Int. J. Cancer* **131**, 2153–2164
20. Awad, O., Yustein, J. T., Shah, P., Gul, N., Katuri, V., O'Neill, A., Kong, Y., Brown, M. L., Toretzky, J. A., and Loeb, D. M. (2010) High ALDH activity identifies chemotherapy-resistant Ewing's sarcoma stem cells that retain sensitivity to EWS-FLI1 inhibition. *PLoS One* **5**, e13943
21. Suvà, M. L., Riggi, N., Stehle, J. C., Baumer, K., Tercier, S., Joseph, J. M., Suvà, D., Clément, V., Provero, P., Cironi, L., Osterheld, M. C., Guillou, L., and Stamenkovic, I. (2009) Identification of cancer stem cells in Ewing's sarcoma. *Cancer Res.* **69**, 1776–1781
22. Scotlandi, K., Manara, M. C., Serra, M., Marino, M. T., Ventura, S., Garofalo, C., Alberghini, M., Magagnoli, G., Ferrari, S., Lopez-Guerrero, J. A., Lombard-Bosch, A., and Picci, P. (2011) Expression of insulin-like growth factor system components in Ewing's sarcoma and their association with survival. *Eur. J. Cancer* **47**, 1258–1266
23. Chang, Y. S., Lee, L. C., Sun, F. C., Chao, C. C., Fu, H. W., and Lai, Y. K. (2006) Involvement of calcium in the differential induction of heat shock protein 70 by heat shock protein 90 inhibitors, geldanamycin and radicicol, in human non-small cell lung cancer H460 cells. *J. Cell. Biochem.* **97**, 156–165
24. Sheng, M., McFadden, G., and Greenberg, M. E. (1990) Membrane depolarization and calcium induce c-fos transcription via phosphorylation of transcription factor CREB. *Neuron* **4**, 571–582
25. Nagamoto-Combs, K., Piech, K. M., Best, J. A., Sun, B., and Tank, A. W. (1997) Tyrosine hydroxylase gene promoter activity is regulated by both cyclic AMP-responsive element and AP1 sites following calcium influx. Evidence for cyclic amp-responsive element binding protein-independent regulation. *J. Biol. Chem.* **272**, 6051–6058
26. Joo, J., Christensen, L., Warner, K., States, L., Kang, H.-G., Vo, K., Lawlor, E. R., and May, W. A. (2009) GLI1 is a central mediator of EWS/FLI1 signaling in Ewing tumors. *PLoS One* **4**, e7608
27. Li, Y. J., Zhao, X., Vecchiarelli-Federico, L. M., Li, Y., Datti, A., Cheng, Y., and Ben-David, Y. (2012) Drug-mediated inhibition of Fli-1 for the treatment of leukemia. *Blood Cancer J.* **2**, e54
28. Akbulut, Y., Gaunt, H. J., Muraki, K., Ludlow, M. J., Amer, M. S., Bruns, A., Vasudev, N. S., Radtke, L., Willot, M., Hahn, S., Seitz, T., Ziegler, S., Christmann, M., Beech, D. J., and Waldmann, H. (2015) (-)-Englerin A is a potent and selective activator of TRPC4 and TRPC5 calcium channels. *Angew. Chem. Int. Ed Engl.* **54**, 3787–3791
29. Miller, M., Shi, J., Zhu, Y., Kustov, M., Tian, J. B., Stevens, A., Wu, M., Xu, J., Long, S., Yang, P., Zholos, A. V., Salovich, J. M., Weaver, C. D., Hopkins, C. R., Lindsley, C. W., et al. (2011) Identification of ML204, a novel potent antagonist that selectively modulates native TRPC4/C5 ion channels. *J. Biol. Chem.* **286**, 33436–33446
30. Deloulme, J. C., Prichard, L., Delattre, O., and Storm, D. R. (1997) The proto-oncoprotein EWS binds calmodulin and is phosphorylated by protein kinase C through an IQ domain. *J. Biol. Chem.* **272**, 27369–27377
31. Kim, J., Lee, J. M., Branton, P. E., and Pelletier, J. (1999) Modification of EWS/WT1 functional properties by phosphorylation. *Proc. Natl. Acad. Sci. U.S.A.* **96**, 14300–14305
32. Park, S., Scheffler, T. L., Rossie, S. S., and Gerrard, D. E. (2013) AMPK activity is regulated by calcium-mediated protein phosphatase 2A activity. *Cell Calcium* **53**, 217–223
33. Mochly-Rosen, D., Das, K., and Grimes, K. V. (2012) Protein kinase C, an elusive therapeutic target? *Nat. Rev. Drug Discov.* **11**, 937–957
34. Rigor, R. R., Hawkins, B. T., and Miller, D. S. (2010) Activation of PKC isoform $\beta(1)$ at the blood-brain barrier rapidly decreases P-glycoprotein activity and enhances drug delivery to the brain. *J. Cereb. Blood Flow Metab.* **30**, 1373–1383
35. Takigami, I., Ohno, T., Kitade, Y., Hara, A., Nagano, A., Kawai, G., Saitou, M., Matsushashi, A., Yamada, K., and Shimizu, K. (2011) Synthetic siRNA targeting the breakpoint of EWS/Flil-1 inhibits growth of Ewing sarcoma xenografts in a mouse model. *Int. J. Cancer* **128**, 216–226
36. Maksimenko, A., and Malvy, C. (2005) Oncogene-targeted antisense oligonucleotides for the treatment of Ewing sarcoma. *Expert Opin. Ther. Targets* **9**, 825–830
37. Toretzky, J. A., Connell, Y., Neckers, L., and Bhat, N. K. (1997) Inhibition of EWS-FLI-1 fusion protein with antisense oligodeoxynucleotides. *J. Neurooncol.* **31**, 9–16
38. Folmer, F., Jaspars, M., Dicato, M., and Diederich, M. (2008) Marine natural products as targeted modulators of the transcription factor NF- κ B. *Biochem. Pharmacol.* **75**, 603–617
39. Hegde, N. S., Sanders, D. A., Rodriguez, R., and Balasubramanian, S. (2011) The transcription factor FOXM1 is a cellular target of the natural product thiostrepton. *Nat. Chem.* **3**, 725–731
40. Kumar, H., Kim, I. S., More, S. V., Kim, B. W., and Choi, D. K. (2014) Natural product-derived pharmacological modulators of Nrf2/ARE pathway for chronic diseases. *Nat. Prod. Rep.* **31**, 109–139
41. Ríos, J. L., Recio, M. C., Escandell, J. M., and Andújar, I. (2009) Inhibition of transcription factors by plant-derived compounds and their implications in inflammation and cancer. *Curr. Pharm. Des.* **15**, 1212–1237
42. Schomburg, C., Schuehly, W., Da Costa, F. B., Klempnauer, K. H., and Schmidt, T. J. (2013) Natural sesquiterpene lactones as inhibitors of Myb-dependent gene expression: structure-activity relationships. *Eur. J. Med. Chem.* **63**, 313–320
43. Yee, D., Favoni, R. E., Lebovic, G. S., Lombana, F., Powell, D. R., Reynolds, C. P., and Rosen, N. (1990) Insulin-like growth factor I expression by tumors of neuroectodermal origin with the t(11;22) chromosomal translocation: a potential autocrine growth factor. *J. Clin. Invest.* **86**, 1806–1814
44. Cironi, L., Riggi, N., Provero, P., Wolf, N., Suvà, M.-L., Suvà, D., Kindler, V., and Stamenkovic, I. (2008) IGF1 is a common target gene of Ewing's sarcoma fusion proteins in mesenchymal progenitor cells. *PLoS One* **3**, e2634
45. Subbiah, V., and Kurzrock, R. (2012) Ewing's sarcoma: overcoming the therapeutic plateau. *Discov. Med.* **13**, 405–415
46. Sourbier, C., Scroggins, B. T., Ratnayake, R., Prince, T. L., Lee, S., Lee, M. J., Nagy, P. L., Lee, Y. H., Trepel, J. B., Beutler, J. A., Linehan, W. M., and Neckers, L. (2013) Englerin A stimulates PKC θ to inhibit insulin signaling and to simultaneously activate HSF1: pharmacologically induced synthetic lethality. *Cancer Cell* **23**, 228–237

Englerin A Inhibits EWS-FLI1 DNA Binding in Ewing Sarcoma Cells
Vittorio Caropreso, Emad Darvishi, Thomas J. Turbyville, Ranjala Ratnayake, Patrick J. Grohar, James B. McMahon and Girma M. Woldemichael

J. Biol. Chem. 2016, 291:10058-10066.

doi: 10.1074/jbc.M115.701375 originally published online March 9, 2016

Access the most updated version of this article at doi: [10.1074/jbc.M115.701375](https://doi.org/10.1074/jbc.M115.701375)

Alerts:

- [When this article is cited](#)
- [When a correction for this article is posted](#)

[Click here](#) to choose from all of JBC's e-mail alerts

This article cites 46 references, 11 of which can be accessed free at
<http://www.jbc.org/content/291/19/10058.full.html#ref-list-1>